International Journal of Education and Science Research Review
E-ISSN 2348-6457
Volume-10, Issue-5 Sep - Oct – 2023
P-ISSN 2349-1817
www.ijesrr.org
Email- editor@ijesrr.org

COST EFFECTIVE METAL AND METAL FREE DYES FOR SOLAR ENERGY HARVESTING

Jyoti Malik
Research Scholar JJT University

Dr. Suprita
Assistant Professor In Department Of Chemistry
JJT university

ABSTRACT

It is important to note that, as was touched on briefly in the paragraphs that came before this one, the efforts that have been made toward developing more environmentally friendly materials have been more focused on individual components (such as the sensitizer, redo couple, electrolyte, and counter-electrode) rather than full devices. In point of fact, zinc-based porphyries demonstrated remarkable photo conversion efficiencies when coupled with cobalt- or iodine-based redo couples (while dissolved in an organic and highly volatile solvent). On the other hand, copper complexes and/or water environments were not taken into consideration. On the other hand, when CRM-free redo couples and aqueous DSSCs were analyzed, neither environmentally neither friendly sensitizers nor counter-electrodes based on platinum were used. Therefore, a strategy that is more thorough is required, with the primary aim being the creation of a device that is both entirely sustainable and cost-effective.

KEYWORDS:- *cost-effective,* energy

INTRODUCTION

We need to find an appropriate response to the question of how humanity will be able to fulfill its energy needs in the near future in light of the fact that the population of the world is about to reach eight billion people and there are projections that the number could even reach ten billion by the middle of this century. To this day, the majority of the world's electricity production is dependent on fossil fuels, which, in addition to being a non-renewable resource, also produce significant quantities of carbon dioxide. Carbon dioxide is a greenhouse gas that has recently emerged as a significant risk to the health of our planet's ecosystem. According to the findings of the Intergovernmental Panel on Climate Change (IPCC), the sector of the economy that deals with the provision of energy is the one that is responsible for the most greenhouse gas emissions worldwide (considering energy extraction, conversion, storage, transmission and distribution processes that deliver final energy to end-use sectors). Within the context of climate change, reducing carbon emissions from the production of electricity is an essential component of developing cost-effective mitigation methods for attaining low-stabilization levels (430–530 pap CO2 equivalent).). In accordance with the Sustainable Development Goal 7 (SDG7, Affordable and Clean Energy) recommendation and the 2030 Climate & Energy Framework, the European Union (EU) has set its sights on achieving the following two goals by the year 2030: I at least a 32 percent share for renewable

energy; and (ii) at least a 32.5 percent improvement in energy efficiency. Both of these goals are outlined in the following sentence.

Because of the high cost of production, financing institutions viewed renewable (such as first-generation solar cells made of ultrapure silicon metal) as risky for a number of years, which resulted in high lending rates for individuals and businesses that needed funding for renewable power generation. However, according to the most recent report published by the International Renewable Energy Agency (IRENA), this trend has been steadily decreasing over the course of the past decade. Furthermore, unsubsidized onshore wind and solar renewable are becoming more and more cost-competitive, and a growing number of businesses are entering the renewable energy industry. Specifically, the report found that the global weighted-average cost of electricity for concentrated solar power (CSP) decreased by 26 percent year-on-years. This was followed by bioenergy, which saw a decrease of 14 percent, solar photovoltaic's (PV), and onshore wind, both of which saw a decrease of 13 percent, hydropower, which saw a decrease of 12 percent, geothermal, and offshore wind, both of which saw a decrease of 1 percent. As a consequence of this, it is anticipated that wind and solar will account for at least half of the world's total power output by the year 2050 due to the decreased cost of renewable energy sources and batteries.

OBJECTIVE

1. To study the low-cost metal and metal-free dyes for solar energy collecting.

2. To study the implementation of fossil fuel laws.

RESEARCH METHODOLOGY

MATERIALS

The majority of the analytical grade reagents and solvents required to carry out the experiments were acquired from Spectrochem, Sigma-Aldrich, and CDH respectively. Laboratory grade reagents were utilized throughout the chromatographic processes that were utilized in order to purify intermediates, products, and final products. In order to conduct spectroscopic research, spectroscopic grade toluene and DMF are purchased from Sigma-Aldrich and utilized in the form in which they were delivered. Column chromatography was performed using silica gel (60-120 mesh), and thin-layer chromatography was carried out using a Merck-percolated silica gel 60-F254 plate. The majority of the reactions were carried out in an atmosphere containing N2 while employing solvents that were dry and degassed, and the crude products were cleaned up using gravity chromatography.

Aldehydes such as tolualdehyde, benzaldehyde, p-hydroxybenzaldehyde, 4- formal moronic acid, ethanylbenzaldehyde and aldehydes of imidazole derivatives such as 4-(1-HImidazolyl) benzaldehyde and amino acids such as arccosine and reagents such as borontribromide (1M in CH Before being put to use, the parole that was obtained from Otto Chemicals was subjected to distillation. CDH Chemicals was the supplier for the glacial acetic acid, prop ionic acid, nitrobenzene, zinc acetate, and ammonium acetate that were acquired. TCI Chemicals was the vendor for the acquisition of fullerenes (C60 and C70).

In order to carry out reactions, solvents of an AR grade were utilized. These solvents included dichloromethane (DCM), chloroform, dimethylformamide (DMF), and acetonitrile. Before being distilled, these solvents were dried over calcium hydride (CaH2) and placed in an environment with inert conditions. After many rounds of

refluxing with sodium metal (Na) and benzophenone, the solvents such as tetrahydrofuran and toluene were evaporated using distillation of the solvent. In order to achieve a higher level of purity, trim ethylamine was refined using sodium hydroxide pellets. Following distillation and purification, the solvents were placed in an inert environment for storage, and molecular sieves with a size of 4 were utilized to ensure that the environment remained dry and degassed.

General

The Broker Advances NMR spectrometer operating at 500 MHz was utilized in order to carry out the characterization of each chemical. Studies of optical absorption were carried out using an Agilent Technologies UV-visible spectrophotometer model Cary 50. The Perkin Elmer LS 55 spectrometer was utilized in the conduct of the fluorescence investigations.

Computational Studies

All of the computations were performed on high-speed personal computers using a software called Gaussian 09. Using the hybrid functional B3LYP156 and the basis set 6-31G, the ground state geometries of all three dyads were optimized to a real global minimum. 157 To determine the steady-state characteristics of the dyads, a TD-DFT B3LYP 6-31G basis set was used, and the polarizable continuum model was used for support. The calculations were done with toluene as the solvent. With the help of the Gauss Sum programmed, the theoretical absorption spectra of the dyads have been calculated.

Fluorescence Up-conversion and Transient Absorption

Studies of femtosecond fluorescence up conversion and transient absorption are discussed elsewhere in detail, along with the experimental setup of these measurements. "A picoseconds time-correlated single photon counting (TCSPC) setup (FluoroLog3-Triple Illuminator, IBH Horiba JobinYvon)" was used to record the fluorescence life times of dyads in various solvents. This setup contained a picoseconds light emitting diode laser (Annulled, ex = 375 for BBA moiety) as the excitation source. In order to record the decay curves, the fluorescence emission maxima at 410 nm (for the BBA moiety) were observed. The decay curves were then evaluated using "non-linear least-squares iteration process utilizing IBH DAS6 (version 2.3) decay analysis software." As a detector, a photomultiplier tube manufactured by Hamamatsu with the model number R928P was employed, and the lamp profile was recorded by substituting a scattered made up of a diluted solution of lido dissolved in water for the sample. The full width at half maximum (FWHM) of the excitation source, which was around 625 pHs at 405 nm, acted as a constraint on the width of the instrument function.

RESULTS

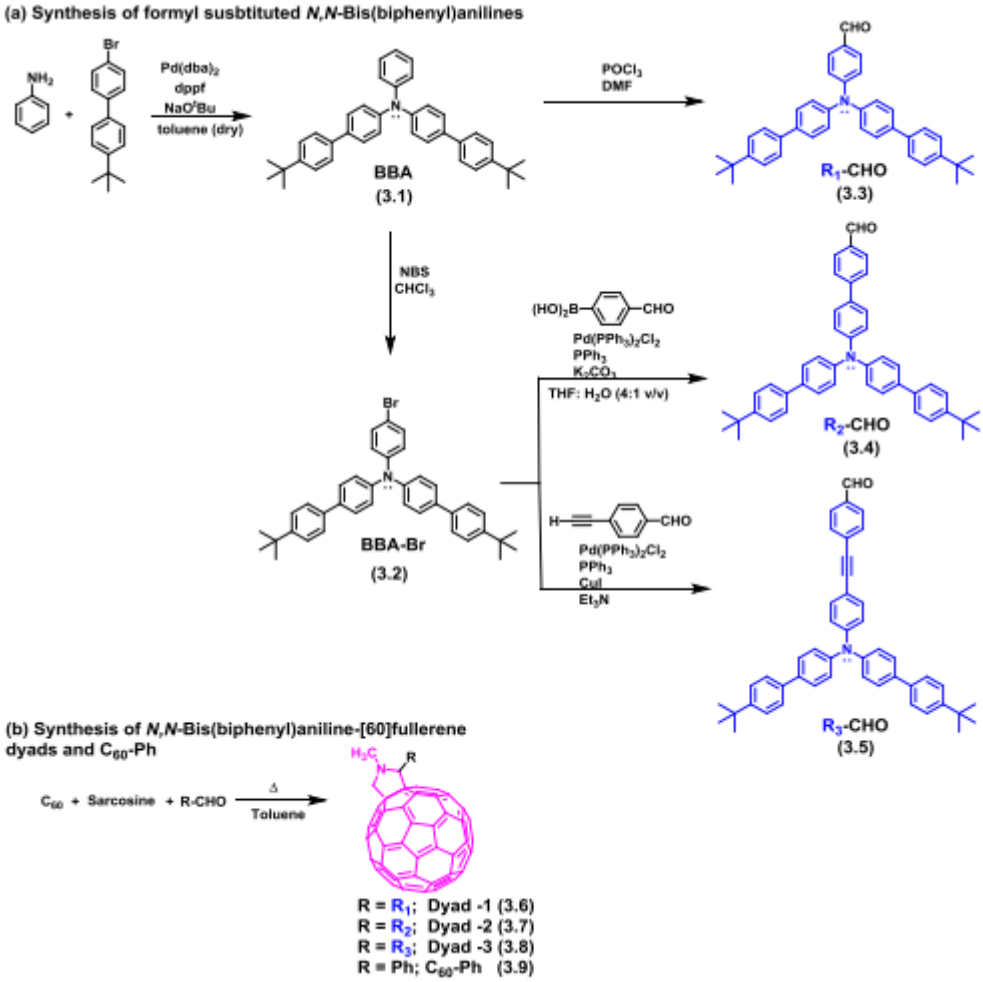

Scheme : Synthetic scheme of BBA-[C60] Fullerene dyads.

Synthesis

Scheme 3.1 provides an overview of the synthesis of BBA-C60 dyads, including Dyads 1-3, which was utilized for the current investigation. In the beginning, the synthesis of BBA, number 3.1, was accomplished by reacting 4-bromo4-tert-butylbiphenyl with aniline in the presence of a Pd(dba)2 catalyst. After that, the compound 3.2 was obtained by brominating 4-bromo-4-tert-butylbiphenyl with NBS. In order to get the chemical R1-CHO, the formulation of BBA was accomplished by performing a typical Vilsmeier-Haack reaction with the use of DMF and POCl3. The substituted BBAs, R2-CHO and R3-CHO, were produced by reacting 4-formylphenylboronic acid or 4-ethynylbenzaldehyde in the presence of Pd catalysts under Suzuki or Sonogashira coupling conditions, respectively. Both of these reactions took place in the presence of Pd catalysts. The next step was the synthesis of the BBA-C60 dyads using the conventional Prato's fulleropyrrolidine synthesis. This involved the condensation of R1-CHO, R2-CHO, and R3-CHO with fullerene in the presence of arccosine, which resulted in the formation of the Dyad-1, Dyad-2, and Dyad-3, respectively. In a similar manner, the control chemical known as C60-Ph was produced by carrying out Prato's reaction with benzaldehyde functioning in the capacity of an aldehyde congener. Methods such as 1H NMR, MALDI-MS, and UV-visible spectroscopic analysis were utilized in order to carry out preliminary characterization of the dyads as well as the control compounds. The MALDI-MS spectra of Dyad-1 exhibited a peak at m/z = 1286 (M+, C101H44N2), the MALDI-MS spectrum of Dyad-2 showed a peak at m/z = 1361.91 (M+, C107H48N2),

and the MALDI-MS spectrum of Dyad-3 m/z = 1385.45 (M+, C109H48N2), which may be attributed to their respective Figures S3.1 through S3.16 show the 1H NMR and 13C NMR spectra of compounds 3.1 through 3.5 and 3.9, as well as the spectra of Dyad-1, Dyad-2, and Dyad-3. Figures S3.17 through S3.25 display the MALDI-MS spectra of dyads.

Electrochemical Measurements

Isolated BBA and C60 were put through cyclic voltammeter tests in 1,2-dichlorobenzene (DCB) as the solvent and NBu4BF4/TBAPF6 as the supporting electrolyte. These tests were carried out so that the reaction free energy for electron transfer could be calculated, as well as the redo properties of all dyads and the control compounds. All potentials are presented vs standard calomel electrode. Isolated BBA demonstrated a single reversible one-electron oxidation wave at a potential of +0.7 V vs SCE, whereas C60 demonstrated three successive reversible one-electron reduction waves, the first of which occurred at a potential of -0.6 V versus SCE (Figure 4.2). In the case of the dyads, i.e., after covalently tethering the BBA to the C60 moiety, a positive shift of +0.16 V in the redo cycle of the BBA moiety is observed without any loss of reversibility, and it is independent of the distance between the BBA and the C60. On the other hand, there was no shift in the redo cycle of the C60 moiety that was observed. The presence of stable radical ions in dyad systems may be inferred from the fact that the redo cycle of the dyads has a high degree of reversibility. Because there is no shift in the reduction wave of the C60 moiety, the positive shift of the oxidation wave of the BBA moiety in dyads may be attributed to a minor interaction between the BBA moiety and the spacer bridge in the ground state. However, this cannot be attributed to the prominent interaction that occurs between the BBA moiety and the C60 moiety.

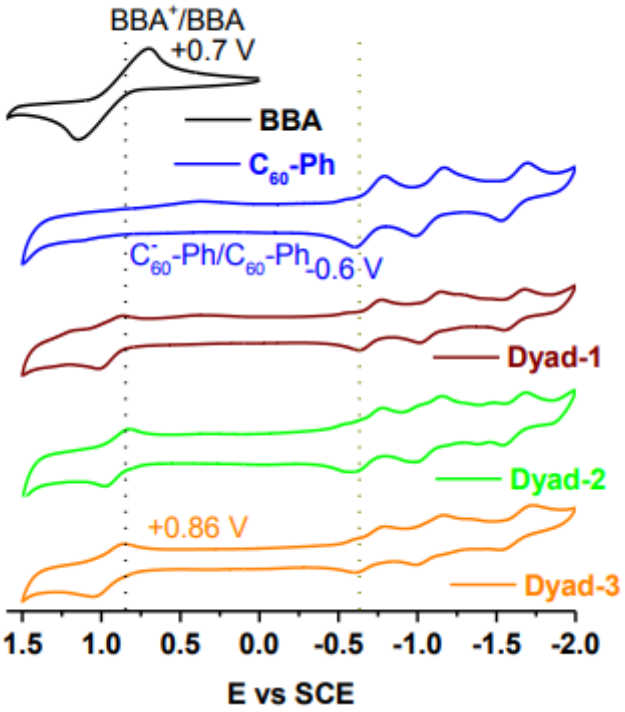

Figure 1: Cyclic voltammograms of BBA, C60-Ph and all three dyads in 1,2-DCB 0.1 M NBu4BF4 as supporting electrolyte.

Thermodynamic free energy, the driving force of electron transfer, for charge-separation (- GCR) have been estimated in toluene and 1:1GCS) as well as charge-recombination (- toluene:DMF mixture for both oxidative electron transfer, excited donor (1BBA*) to ground state acceptor (C60), and reductive electron transfer, ground state donor (BBA) to excited acceptor (C60), within the framework work of

$$\Delta G_{CS} = e(E_{OX} - E_{red}) - \Delta E^{S}_{0,0} - \frac{e^2}{4\pi\epsilon_0\epsilon_S R_{CC}}$$

$$\Delta G_{CR} = -e(E_{OX} - E_{red}) + \frac{e^2}{4\pi\epsilon_0\epsilon_S R_{CC}}$$

Where $\Delta E^{S}_{0,0}$ the 0-0 fluorescence transition energy and RCC is is the centre-to-centre distance between donor and acceptor, e is the charge of electron and ε_S is dielectric constant of solvent. The value of $\Delta E^{S}_{0,0}$ Depending on the polarity of the solvent, the energy required for oxidative electron transfer can range from 3.2 to 3.05 eV (fluorescence emission peak, 1BBA*), whereas the energy required for reductive electron transfer is 1.75 eV (fluorescence emission peak, 1C60 *). CS is an energetically downhill and spontaneous process in both oxidative and reductive pathways, whereas in toluene, CS is energetically possible only via oxidative path while reductive path is endothermic in nature. The estimated values that are listed in Table 1. suggest that formation of photoinduced charge-separated (CS) state is exergonic in 1:1 mixture of toluene and DMF. This is illustrated by the fact that CS is exergonic

Table 1: Electrochemical dataa of all three dyads and isolated donor (BBA) and acceptor (C60-Ph).

System	E_{ox} (V)	E_{red} (V)	Oxidative -ΔG_{CS} (eV)		Reductive-ΔG_{CS} (eV)		-ΔG_{CR} (eV)	
			Toluene	1:1 (Tol:DMF)[c]	Toluene	1:1 (Tol:DMF)[c]	Toluene	1:1 (Tol:DMF)[c]
BBA,C_{60}-Ph	0.93[b]	-0.71[b]	1.23[c]	1.67[d]	-0.24[d]	0.37[d]	1.94[d]	1.43[d]
Dyad-1	0.94	-0.70	1.47	1.70	0.01	0.35	1.73	1.40
Dyad-2	0.93	-0.69	1.29	1.7	-0.11	0.35	1.91	1.42
Dyad-3	0.94	-0.71	1.16	1.66	-0.31	0.31	2.04	1.42

a calculated as the average of Eox and Ered b redox potentials of isolated BBA and C60, c the dielectric constant of a mixture of 1:1 toluene and DMF is assumed to be the average of the dielectric constants of the individual solvents, and d the radii of BBA and C60 are found to be 6 (R+) and 4.2 (R-) from the MO calculation.

CONCULSION

The process of artificial photosynthesis is a man-made process that imitates the natural process of photosynthesis in order to transform light energy into a variety of different types of energy such as chemical energy, electrical energy, and fuels. A typical artificial photosynthetic system is made up of a number of antenna molecules that are made up of chromophores that absorb solar energy over a wide range of wavelengths and transfer that energy to the primary electron donor(s) through photo-induced energy transfer (PEnT), which then

transfers its energy via photo-induced electron transfer (PET) to the electron acceptor(s) and achieves the long-lived charge separated (CS) states. The research work that went into designing, synthesizing, characterizing, and determining the photo physical and electrochemical properties of several artificial photosynthetic models that can be used to design solar energy harvesting devices has been discussed in this thesis. These models can be used as inspiration for the design of these devices. The first chapter provides a concise summary of the various donor-acceptor systems along with their photo physical characteristics and discusses how the scientific community has applied these concepts in order to build light harvesting systems that have the potential to be utilized in solar cells. The second chapter covers a variety of photo physical approaches that were utilized in order to monitor the PET and PEnT processes that were taking place in the donor-acceptor systems that were detailed in the thesis.

REFERENCES

(1) Cairney, P.; McHarg, A.; McEwen, N.; Turner, K. Energy Policy 2019, 129, 459.

(2) Conti, J.; Holtberg, P.; Diefenderfer, J.; LaRose, A.; Turnure, J. T.; Westfall, L. International energy outlook 2016 with projections to 2040, USDOE Energy Information Administration (EIA), Washington, DC (United States …, 2016).

(3) Meinshausen, M.; Meinshausen, N.; Hare, W.; Raper, S. C.; Frieler, K.; Knutti, R.; Frame, D. J.; Allen, M. R. Nature 2009, 458, 1158.

(4) Aizebeokhai, A. International Journal of Physical Sciences 2009, 4, 868.

(5) Panwar, N.; Kaushik, S.; Kothari, S. Renewable and Sustainable Energy Reviews 2011, 15, 1513.

(6) Yang, Y.; Solgaard, H. S.; Haider, W. Energy Policy 2016, 97, 521.

(7) Lewis, N. S. science 2007, 315, 798.

(8) Deisenhofer, J. The Photosynthetic Reaction Center 1993, 541.

(9) Blankenship, R. E. Molecular mechanisms of photosynthesis; John Wiley & Sons, 2014.

(10) Umena, Y.; Kawakami, K.; Shen, J.-R.; Kamiya, N. Nature 2011, 473, 55.

(11) Fleming, G. R.; Schlau-Cohen, G. S.; Amarnath, K.; Zaks, J. Faraday discussions 2012, 155, 27.

(12) Karkas, M. D.; Verho, O.; Johnston, E. V.; Åkermark, B. r. Chemical reviews 2014, 114, 11863.